

The *Aspergillus fumigatus* Damage Resistance Protein Family Coordinately Regulates Ergosterol Biosynthesis and Azole Susceptibility

Jinxing Song,^a Pengfei Zhai,^a Yuanwei Zhang,^a Caiyun Zhang,^b Hong Sang,^b Guanzhu Han,^a Nancy P. Keller,^c Ling Lu^a

Jiangsu Key Laboratory for Microbes and Functional Genomics, Jiangsu Engineering and Technology Research Center for Microbiology, College of Life Sciences, Nanjing Normal University, Nanjing, China^a; Department of Dermatology, Jinling Hospital, School of Medicine, Nanjing University, Nanjing, China^b; Department of Bacteriology and Department of Medical Microbiology and Immunology, UW-Madison, Madison, Wisconsin, USA^c

ABSTRACT Ergosterol is a major and specific component of the fungal plasma membrane, and thus, the cytochrome P450 enzymes (Erg proteins) that catalyze ergosterol synthesis have been selected as valuable targets of azole antifungals. However, the opportunistic pathogen *Aspergillus fumigatus* has developed worldwide resistance to azoles largely through mutations in the cytochrome P450 enzyme Cyp51 (Erg11). In this study, we demonstrate that a cytochrome *b*₅-like heme-binding damage resistance protein (Dap) family, comprised of DapA, DapB, and DapC, coordinately regulates the functionality of cytochrome P450 enzymes Erg5 and Erg11 and oppositely affects susceptibility to azoles. The expression of all three genes is induced in an azole concentration-dependent way, and the decreased susceptibility to azoles requires DapA stabilization of cytochrome P450 protein activity. In contrast, overexpression of DapB and DapC causes dysfunction of Erg5 and Erg11, resulting in abnormal accumulation of sterol intermediates and further accentuating the sensitivity of Δ *dapA* strains to azoles. The results of exogenous-hemin rescue and heme-binding-site mutagenesis experiments demonstrate that the heme binding of DapA contributes the decreased azole susceptibility, while DapB and -C are capable of reducing the activities of Erg5 and Erg11 through depletion of heme. *In vivo* data demonstrate that inactivated DapA combined with activated DapB yields an *A. fumigatus* mutant that is easily treatable with azoles in an immunocompromised mouse model of invasive pulmonary aspergillosis. Compared to the single Dap proteins found in *Saccharomyces cerevisiae* and *Schizosaccharomyces pombe*, we suggest that this complex Dap family regulatory system emerged during the evolution of fungi as an adaptive means to regulate ergosterol synthesis in response to environmental stimuli.

IMPORTANCE Knowledge of the ergosterol biosynthesis route in fungal pathogens is useful in the design of new antifungal drugs and could aid in the study of antifungal-drug resistance mechanisms. In this study, we demonstrate that three cytochrome *b*₅-like Dap proteins coordinately regulate the azole resistance and ergosterol biosynthesis catalyzed by cytochrome P450 proteins. Our new insights into the Dap regulatory system in fungal pathogens may have broad therapeutic ramifications beyond their usefulness for classic azole antifungals. Moreover, our elucidation of the molecular mechanism of Dap regulation of cytochrome P450 protein functionality through heme-binding activity may extend beyond the Kingdom Fungi with applicability toward Dap protein regulation of mammalian sterol synthesis.

Received 19 November 2015 Accepted 14 January 2016 Published 23 February 2016

Citation Song J, Zhai P, Zhang Y, Zhang C, Sang H, Han G, Keller NP, Lu L. 2016. The *Aspergillus fumigatus* damage resistance protein family coordinately regulates ergosterol biosynthesis and azole susceptibility. *mBio* 7(1):e01919-15. doi:10.1128/mBio.01919-15.

Editor John W. Taylor, University of California **Invited Editor** Gustavo H. Goldman, Universidade de Sao Paulo

Copyright © 2016 Song et al. This is an open-access article distributed under the terms of the [Creative Commons Attribution-NonCommercial-ShareAlike 3.0 Unported license](https://creativecommons.org/licenses/by-nc-sa/4.0/), which permits unrestricted noncommercial use, distribution, and reproduction in any medium, provided the original author and source are credited.

Address correspondence to Ling Lu, linglu@njnu.edu.cn.

Sterols are major components of most eukaryotic plasma membranes and have been shown to be responsible for a number of biological functions, such as membrane fluidity and the functions of integral membrane proteins (1–6). Eukaryotic kingdoms differ in the precise structure of sterols such that animals synthesize cholesterol, plants synthesize sitosterol, campesterol, and stigmasterol, and fungi synthesize mainly ergosterol. Common to all sterols is having the saturated bond at C-5,6 and the presence of the hydroxyl group at C-3. Ergosterol differs from cholesterol by the presence of unsaturated bonds at C-7,8 in the ring structure and C-22 in the side chain and by the presence of a methyl group at C-24 on the side chain (7). Thus, ergosterol biosynthetic compo-

nents specific to fungi have been selected as the targets for most of the antifungal compounds currently used in agricultural settings and in combating human infections.

A valuable class of antifungals, the azoles, specifically target Cyp51 (Erg11), a cytochrome P450 monooxygenase also known as lanosterol demethylase, which is critical for ergosterol synthesis (8). Cytochrome P450 proteins are characterized by the spectral absorbance of a cysteine-linked heme molecule at the active site (9, 10). The human pathogen *Aspergillus fumigatus* contains two Cyp51 (Erg11A and -B [Erg11A/B]) paralogs, encoded by *erg11A* (Afu4g06890) and *erg11B* (Afu7g03740), that are 60% homologous with each other and act in a compensatory manner in the

ergosterol biosynthesis pathway (11). It is postulated that *cyp51A* (*erg11A*) may encode the major sterol 14- α -demethylase (12), with Cyp51B (*Erg11B*) either being functionally redundant or having an alternative function under particular unknown growth conditions (13, 14). Both Cyp51 paralogs locate to the endoplasmic reticulum, and deletion of both genes is required for lethality (14). Over the last few decades, the most common mechanism of resistance to azole antifungals observed in *A. fumigatus* samples isolated in the clinical and environmental milieu is related to point mutations in Cyp51A (*Erg11A*) (15, 16), called hot spots, that alter the drug-enzyme interaction. Mutations in Cyp51A (*Erg11A*) may directly restrict the docking of the drug, reduce the affinity of the target by altering the structure of the opening in each molecule, or change the position of the heme-binding molecule (17). Therefore, itraconazole (ITZ) and voriconazole (VOR), commonly used as the first-choice therapies for acute allergic aspergillosis or invasive aspergillosis because of their limited side effects in the host (18), are increasingly less efficacious for treatment of *A. fumigatus* infections.

Dap1 (damage resistance protein 1) was first identified in the budding yeast *Saccharomyces cerevisiae* in relation to DNA damage resistance (19–21). Dap1 is a predicted 25-kDa protein that is comprised largely of a heme 1 domain and has significant homology with cytochrome *b*₅, which positively regulates some reactions catalyzed by cytochrome P450 proteins (22). Cytochrome *b*₅ contains protoporphyrin IX, which possibly serves as an electron transfer link between NADH and cytochrome *c* and is known to be involved as an electron transfer component in a number of oxidative reactions in biological tissues (23). Several studies have indicated that a Dap1 defect partially arrests sterol synthesis at the stage catalyzed by *Erg11* (19). In addition, Dap1 predominantly localizes to vacuole membranes and endosomes and mediates a functional link between sterol synthesis and iron homeostasis in yeasts (10). To date, the Dap1 homolog in the filamentous fungus *A. fumigatus* has not been identified. Based on a genome-scale homologue search, we find that most fungal pathogen genomes contain three Dap proteins, but notably, the nonpathogenic yeasts *Schizosaccharomyces pombe* and *Saccharomyces cerevisiae* contain only one Dap protein. We ask what the significance of the Dap proteins is for sterol biosynthesis and azole susceptibility in pathogens, including the three copies of Dap proteins. Answering these questions may yield promising and unexpected insights into the understanding of the molecular mechanisms involved in the regulation of the ergosterol biosynthesis pathway and azole resistance.

Here, we find that in *A. fumigatus*, three members of the Dap family, DapA, DapB, and DapC, all share a conserved cytochrome *b*₅-like heme-binding domain. DapA predominantly controls susceptibility to azoles by stabilizing two cytochrome P450 ergosterol biosynthesis enzymes, *Erg11* and *Erg5*, while DapB and DapC have roles opposite to that of DapA through competitive heme binding that leads to loss of *Erg5* and *Erg11* activity. Consequently, overexpression of DapB or DapC exacerbates azole susceptibility and induces a severely abnormal ergosterol biosynthesis profile in the absence of DapA. Our *in vivo* data demonstrate that the Dap family proteins coordinately regulate azole susceptibility in an immunocompromised mouse model of invasive pulmonary aspergillosis.

RESULTS

Three predicted yeast *dap1* orthologs, *dapA*, -*B*, and -*C*, in *A. fumigatus* respond to azole stress. Based on the sequences of Dap protein family members retrieved from the NCBI Reference Sequence Database for fungi and the Ensembl Genome Browser for humans and mice, using the BLAST algorithm with a cutoff value of 10⁻⁵, a genome-scale homologue search showed that the *S. pombe* genome encodes only one copy of the Dap protein (i.e., Dap1 or DapA), as does the genome of *S. cerevisiae*. However, most fungal pathogens and filamentous fungi encode three Dap proteins, referred to as DapA, DapB, and DapC. Putative DapB and -C homologs are present in mammalian genomes, while DapA is specific to fungi (see Fig. S1 in the supplemental material). Similar to all fungal pathogen species selected, there are three predicted Dap homologs in *A. fumigatus* (GenBank accession numbers XP_754570, XP_753017, and XP_752200) that share high sequence similarity to *S. cerevisiae* Dap1, especially in the cytochrome *b*₅-like heme-binding domain, but low homology with a mammalian homolog, the membrane-associated progesterone receptor. Subsequent BLAST analysis in the *S. cerevisiae* genome database using the *A. fumigatus* sequences with GenBank accession numbers XP_754570, XP_753017, and XP_752200 as queries identified Dap1 as the top hit, suggesting that these *A. fumigatus* sequences and Dap1 are potential orthologs. We consequently named these three proteins DapA (GenBank sequence accession number XP_754570), DapB (GenBank sequence accession number XP_752200), and DapC (GenBank sequence accession number XP_753017). On the basis of the full-length sequences, DapA, DapB, and DapC contain 155, 127, and 243 amino acid residues and display 49%, 36%, and 38% sequence similarity, respectively, to *S. cerevisiae* Dap1. Moreover, according to SMART protein and TMHMM transmembrane analysis, all three predicted Dap proteins contain the cytochrome *b*₅-like heme-binding domain, but only DapA has a predicted transmembrane domain, which starts at position 7 and ends at position 24 of the DapA protein sequence (Fig. 1A).

To test whether these three predicted Dap family members could respond to azole stresses, we next generated strains SJX01, SJX02, and SJX03, which express them from their genomes as green fluorescent protein (GFP)-tagged fusion proteins, by inserting the gene for the GFP tag at the end of the gene that encodes the C-terminal end of the product. All of the Dap-GFP transformants identified showed growth phenotypes similar to that of the parental strain, with or without treatment by azole drugs. Next, a Western blotting experiment was carried out to analyze the molecular masses of DapA, -B, and -C. After accounting for GFP as a 27-kDa protein, the relative molecular masses for DapA, -B, and -C were approximately 17, 14, and 27 kDa, respectively (Fig. 1B), consistent with the predicted sizes of the Dap proteins deduced by coding sequence analysis. As a parental control, strain A1160 lacking the GFP tag did not express any detectable bands. To investigate whether Dap family expression changed upon treatment with the antifungal itraconazole (ITZ), we analyzed the expression of all three Dap proteins by Western blotting. Our results showed that the expression of all three Dap proteins increased in a dose-dependent manner in cells treated with 0 to 0.15 μ g/ml ITZ (Fig. 1B). These results indicated that all Dap members are able to respond to azole stress stimuli in *A. fumigatus*. To further address whether the dose-dependent increases in Dap protein levels were

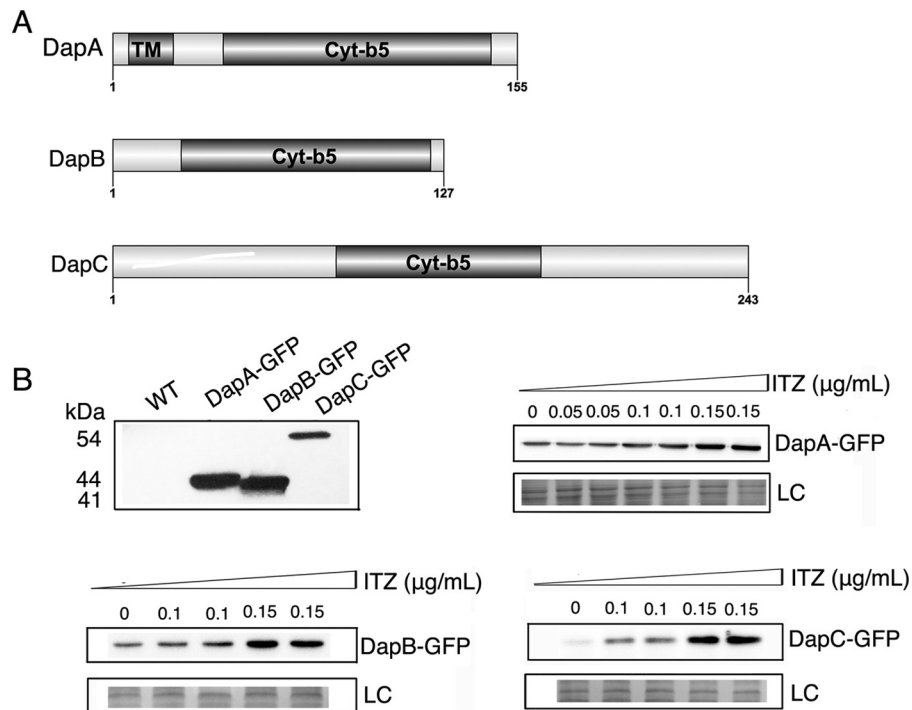


FIG 1 Three predicted yeast Dap1 orthologs, DapA, DapB, and DapC, respond to azole stress stimuli in *A. fumigatus*. (A) Predicted cytochrome b_5 -like heme-binding and transmembrane (TM) domains in DapA, DapB, and DapC, based on a SMART protein search (<http://smart.embl-heidelberg.de/>). (B) DapA-GFP, DapB-GFP, and DapC-GFP fusion proteins with the predicted sizes of about 44, 41, and 54 kDa, respectively (upper left), were found. When the strains expressing the fusion proteins were cultured in ITZ-amended medium, the accumulation of Dap-GFP fusion proteins increased in a dose-dependent manner.

mediated by increases in transcription or in protein stability, we carried out quantitative reverse transcription (qRT)-PCR to test the mRNA abundance in SJX01, SJX02, and SJX03 after exposure to azole treatment. The mRNA levels detected showed that the native promoters of all three of the *dap* genes are able to sense and respond to azole stress stimuli to some extent (see Fig. S2A in the supplemental material). To further test whether the response to azole stress stimuli is related to the promoters of the three *dap* genes, we generated strains SJX04, SJX05, and SJX06, expressing the C-terminally GFP-tagged Dap proteins under the control of the constitutive promoter *gpdA*, originally obtained from *Aspergillus nidulans*. Different from strains in which the Dap proteins were controlled under the native promoter, no significant changes in Dap protein expression under the control of the *gpdA* promoter were observed (see Fig. S2B), suggesting that only the *dap* native promoters are able to sense and respond to azole stress stimuli.

Deletion of *dapA* or *dapC* but not *dapB* causes differing azole susceptibilities. To determine whether Dap proteins affect susceptibility to azoles, *dap* null mutants were generated by homologous recombination in which the *dap* open reading frames (ORFs) were replaced with the *pyr4* selectable marker; the resulting strains were named SJX07 (Δ *dapA*), SJX08 (Δ *dapB*), and SJX09 (Δ *dapC*). Diagnostic PCR confirmed that all three *dap* deletion strains had the correct insertion of the *pyr4* disruption cassette, and no original *dap* ORFs were detected (see Fig. S3 in the supplemental material). We then examined and compared the azole susceptibilities of the deletion mutants and their parental strain. The colony growth phenotypes were observed by spotting a series of 10-fold dilutions of spores onto minimal medium plates

containing 0.3 μ g/ml ITZ. Each deletion strain displayed a different phenotype: the Δ *dapA* strain was hypersensitive to ITZ, the sensitivity of the Δ *dapB* strain to ITZ was indistinguishable from that of the parental strain, and the Δ *dapC* strain was more resistant to ITZ than the parental strain (Fig. 2A). Consistent with the colony growth phenotypes observed on the plates, the Δ *dapA* strain displayed hypersensitivity to ITZ compared with the susceptibility of the parental strain in liquid medium containing 0.2 μ g/ml ITZ, and the Δ *dapC* strain showed more resistance to ITZ than the parental strain in liquid medium containing 0.4 μ g/ml ITZ (Fig. 2A). E-test strips further confirmed that the Δ *dapA* strain showed an approximately fivefold decrease in its ITZ MIC (MIC = 0.38 μ g/ml) compared to the MIC for the parental strain (MIC = 2 μ g/ml). Similar to our results for ITZ, the Δ *dapA* strain also showed increased susceptibility to another azole antifungal, voriconazole (VOR) (MIC = 0.008 μ g/ml), compared to the susceptibility of the parental strain (MIC = 0.064 μ g/ml) (Fig. 2B). Moreover, when the Δ *dapA*, Δ *dapB*, and Δ *dapC* mutants were complemented with their respective native gene, the ensuing strains, named SJX10 (*dapA* reconstituted [*dapA*-recon]), SJX11 (*dapB*-recon), and SJX12 (*dapC*-recon), showed azole susceptibility phenotypes similar to that of the parental strain, indicating that the aberrant Δ *dapA* and Δ *dapC* azole sensitivity phenotypes were specific to the loss of these genes (Fig. 2A). These results suggest that DapA and DapC may mediate azole susceptibility via opposing pathways in *A. fumigatus*.

DapA dominantly contributes to azole resistance, while DapB and DapC negatively mediate this process. Coupling our findings described above with the fact that all of the Dap homologs

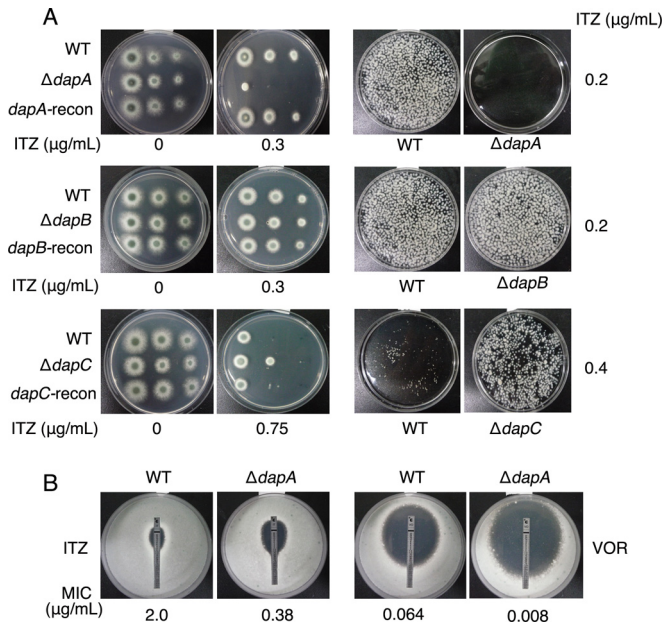


FIG 2 Deletion of *dapA* or *dapC* but not *dapB* causes differing azole susceptibilities. (A) Comparison of ITZ susceptibilities in *dap* null mutants, *dap*-reconstituted mutants, and the parental strains. (Left) Different strains were inoculated as a series of 3- μl 10-fold dilutions derived from a starting suspension of 10^7 conidia per ml onto solid minimal medium (MM) with or without ITZ and cultured at 37°C for 3 days with ITZ or 2 days without ITZ. (Right) For comparison of the susceptibilities of the indicated strains in liquid MM supplemented with ITZ, amounts of 10^8 conidia of Δdap mutants and the parental strain were inoculated into 50 ml of liquid MM supplemented with ITZ and cultured at 37°C with shaking at 220 rpm for 2 days. The cultures were poured into a new petri dish to be photographed. (B) E test strips impregnated with a gradient of ITZ or VOR were placed on MM agar plates containing a lawn grown from conidia of the different strains and cultured for 2 days at 37°C before observation.

share a conserved cytochrome *b*₅-like heme-binding domain, we hypothesized that these proteins may have overlapping functions that could affect azole susceptibility. We therefore transformed the full-length ORF sequence of *dapB* or *dapC* under the control of the *gpdA* promoter into the *dapA* deletion strain and the parental strain separately, resulting in four overexpression (OE) strains that we named SJX13 ($\Delta dapA^{OE::dapB}$), SJX14 (wild type^{OE::dapB}), SJX15 ($\Delta dapA^{OE::dapC}$), and SJX16 (wild type^{OE::dapC}). The expression levels of *dapB* and *dapC* in strains SJX13 ($\Delta dapA^{OE::dapB}$), SJX14 (wild type^{OE::dapB}), SJX15 ($\Delta dapA^{OE::dapC}$), and SJX16 (wild type^{OE::dapC}) were determined by qRT-PCR analysis (see Fig. S4A in the supplemental material), and the results indicated that the mRNA level of *dapB* or *dapC* had been sharply increased in these OE strains. All of the strains contained their native *dapB* and *dapC* alleles. Whereas overexpression of either *dapB* or *dapC* in a *dapA* wild-type background (SJX14 and SJX16 strains) had little impact on sensitivity to azoles, incorporation of these alleles into the $\Delta dapA$ background (SJX13 and SJX15) presented a hypersensitive phenotype on ITZ-amended medium (Fig. 3A). Consistent with the colony growth phenotypes observed on the plates, strains SJX13 and SJX15 also presented a phenotype of hypersensitivity to ITZ in liquid medium (Fig. 3B). E-test strips further confirmed that strains SJX13 and SJX15 strain exhibited increased susceptibility to azoles (Fig. 3C). These observations, which supported the earlier observation that DapC negatively regulated azole resistance (Fig. 2), also suggested that DapB could play a similar role of negative regulation of resistance to azole antifungals.

Next, we asked whether the overexpression of *dapA* in the absence of *dapB* or *dapC* could affect azole susceptibility. To answer this question, we constructed three strains by placing the *dapA* overexpression sequence in the $\Delta dapB$ (SJX17), $\Delta dapC$ (SJX19), and wild-type (SJX18) backgrounds. Strains SJX17 and SJX18 exhibited phenotypes in the presence of ITZ that were similar to that

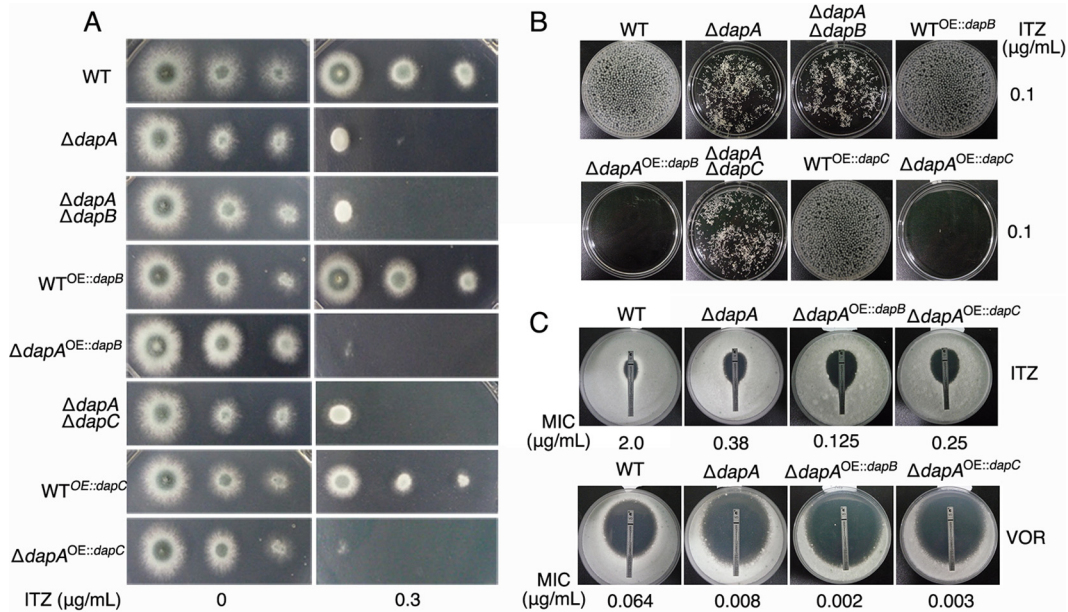


FIG 3 DapA dominantly contributes to azole susceptibility, while overexpression of DapB or DapC negatively mediates this process. (A) Susceptibility comparison of different strains on MM plates supplemented with ITZ (0.3 $\mu\text{g/ml}$) as described in the legend to Fig. 2. (B) Susceptibility comparison of different strains in liquid MM containing ITZ as described in the legend to Fig. 2. (C) E-test strips impregnated with a gradient of ITZ or VOR were placed on MM agar plates containing lawns grown from conidia of different strains and cultured for 2 days at 37°C before observation.

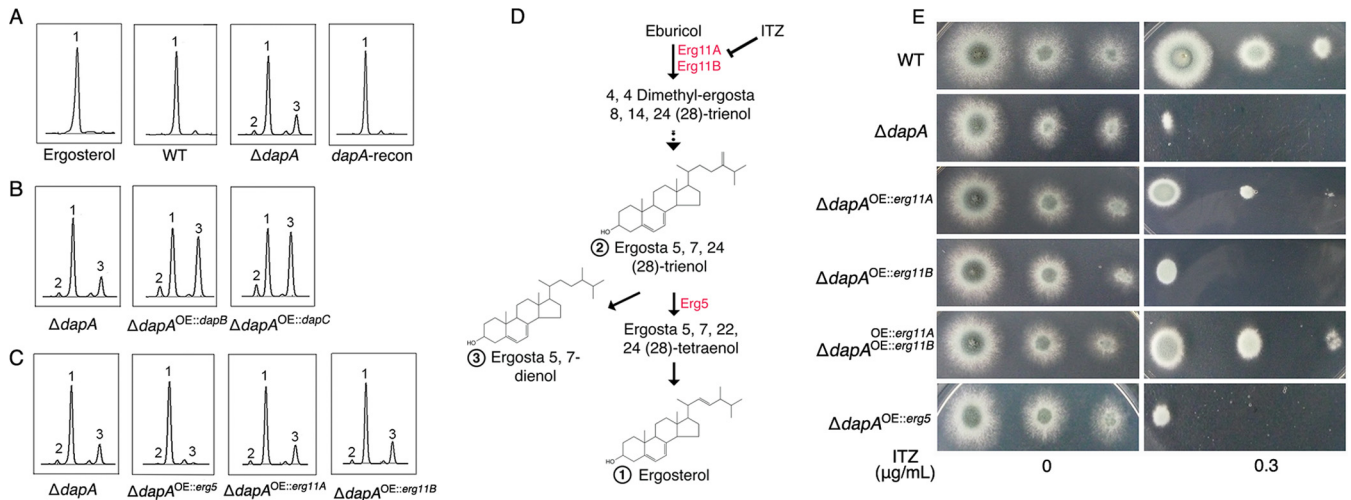


FIG 4 Dap proteins mediate the functions of Erg5 and Erg11. (A to C) The sterol intermediates were analyzed by HPLC and LC-MS/MS. HPLC chromatograms of sterol extracts from the indicated strains and of commercially purified ergosterol are shown. LC-MS/MS analysis identified the elution peaks marked 1, 2, and 3 as ergosterol, ergosta-5,7,24(28)-trienol, and ergosta-5,7-dienol, respectively. (D) A diagram showing the sterol biosynthetic pathway in which the sterol intermediates numbered in A to C and the catalytic enzymes are displayed. (E) Comparison of the ITZ susceptibilities of the indicated strains, showing that overexpression of *erg11A* or *erg11B* or both but not of *erg5* remarkably suppressed the susceptibility of the Δ *dapA* strain to ITZ (0.3 μ g/ml).

of the Δ *dapB* deletion strain, which was equivalent to the wild-type phenotype (Fig. 2). In contrast, the overexpression of *dapA* could partly rescue the resistance phenotype of the *dapC* deletion strain (see Fig. S4B and C in the supplemental material). These findings further strengthen the evidence for opposing activities of DapA and DapC.

To further examine and compare the azole susceptibilities of the *dap* family, we next constructed Δ *dapA* Δ *dapB* and Δ *dapA* Δ *dapC* double deletion mutants through the deletion of *dapB* or *dapC* in the Δ *dapA* strain, yielding two strains named SJX20 (Δ *dapA* Δ *dapB*) and SJX21 (Δ *dapA* Δ *dapC*). Strains SJX20 and SJX21 showed susceptibility profiles similar to that of the Δ *dapA* single mutant (Fig. 3A). These findings indicate that the gain of azole resistance associated with a single *dapC* deletion required an active DapA protein.

Dap proteins mediate the functions of Erg5 and Erg11. The Dap family coordinately affected azole susceptibility, which most likely results from abnormal membrane lipid compositions of fungal cells, because ergosterol biosynthesis is a drug target of ITZ and VOR. To address this possibility, we compared the sterol profiles in the mutants and their parental strains by high-performance liquid chromatography (HPLC). Total sterol was extracted and purified as described previously (24). When using commercial purified ergosterol as a standard, HPLC analysis displayed a single peak at \sim 10.5 min of retention time. In comparison, apart from a predicted component—ergosterol—at \sim 10.5 min of retention time, the sterol profile in the Δ *dapA* strain displayed two additional small peaks that eluted at approximately 9.9 min and 11.8 min, respectively (Fig. 4A). However, the Δ *dapB* and Δ *dapC* strains showed sterol profiles similar to that of the parental control strain. Interestingly, the sterol profiles from strains SJX13 (Δ *dapA* OE::*dapB*) and SJX15 (Δ *dapA* OE::*dapC*) showed two fraction peaks, at retention times of 9.9 min and 11.8 min, that were increased compared with the sterol profile from the parental strain or even that of the Δ *dapA* single mutant strain, as well as showing decreases in the main component, ergosterol, at

\sim 10.5 min of retention time (Fig. 4B). To verify these abnormally enriched components, liquid chromatography-tandem mass spectrometry (LC-MS/MS) analysis was carried out and identified the fractions that eluted at 9.9 min and 11.8 min as ergosta-5,7,24(28)-trienol and ergosta-5,7-dienol, respectively. Based on published information on yeasts, we deduced that the accumulation of these two intermediate products was most likely due to the dysfunction of Erg5, the cytochrome P450 C-22 desaturase (25). We next overexpressed *erg5* in the absence of *dapA* (Δ *dapA* OE::*erg5*) to determine whether it could rescue the abnormal ergosterol biosynthesis profile. As predicted, the accumulation of ergosta-5,7,24(28)-trienol and ergosta-5,7—dienol decreased significantly, especially ergosta-5,7—dienol, which was almost absent in strain SJX22 (Δ *dapA* OE::*erg5*) (Fig. 4C). These data indicate that DapA is required for the normal function of Erg5 during the regulation of the process of ergosterol biosynthesis and that multiple copies of *erg5* could suppress the defect of the *dapA* mutant in ergosterol biosynthesis.

However, surprisingly, overexpression of *erg5* in the SJX22 strain could not rescue the abnormal phenotype of the Δ *dapA* strain in the azole susceptibility test (Fig. 4E), indicating that the loss of *dapA* may affect other Erg enzymes. Considering the likely interaction of Erg11/Cyp51 with DapA and cytochrome P450 enzymes and its role as a direct target of the azole antifungals ITZ and VOR, we hypothesized that the function of Erg11/Cyp51 could also be compromised by *dapA* deletion. Therefore, we next tested whether the overexpression of *erg11A* or *erg11B* was able to suppress the azole sensitivity defect of Δ *dapA* by constructing strains SJX23 (Δ *dapA* OE::*erg11A*) and SJX24 (Δ *dapA* OE::*erg11B*). Unlike strain SJX22, strains SJX23 and SJX24 partly rescued the azole susceptibility in the Δ *dapA* strain. When the Δ *dapA* strain was transformed with both ectopically expressed OE::*erg11A* and OE::*erg11B* alleles, yielding strain SJX25 (Δ *dapA* OE::*erg11A* OE::*erg11B*), the azole susceptibility almost recovered to that of the parental strain (Fig. 4E), indicating that multiple copies of *erg11A* and *erg11B* are capable of suppressing the defect of the Δ *dapA* strain's response to

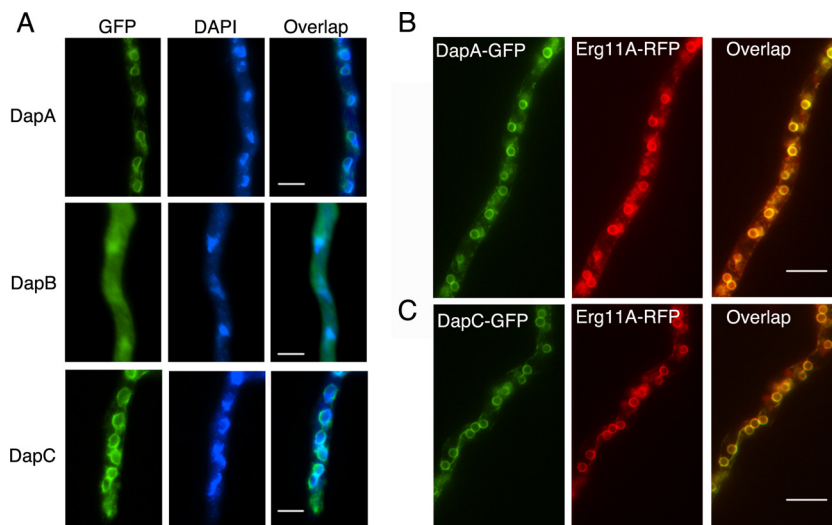


FIG 5 DapA and DapC but not DapB localize in the ER and colocalize with Erg11, as shown by using GFP-tagged fusion proteins. DAPI (4[prime],6-diamidino-2-phenylindole) was used to visualize nuclei. (A) DapA-GFP and DapC-GFP predominantly localize in the ER, while DapB-GFP shows nuclear and cytosolic localization. (B) Colocalization of DapA-GFP or DapC-GFP with Erg11A-RFP is visualized by fluorescence microscopy; the merged image (yellow) shows the high degree of colocalization. Scale bars = 10 μ m.

azole antifungals. In comparison, overexpression of *erg11A* or *erg11B* in the parental wild-type background strain was unable to significantly increase azole resistance under the conditions tested (see Fig. S5A in the supplemental material). These data suggest that DapA contributes to ergosterol synthesis and, hence, decreased azole susceptibility by promoting Erg5 and Erg11 functions.

DapA and DapC but not DapB localized in the ER and colocalized with Erg11. The cellular localization of the Dap proteins as assessed by microscopic observations showed that DapA-GFP and DapC-GFP were predominantly localized in the endoplasmic reticulum (ER), with a network of strands around the peripheral nuclear envelope (Fig. 5A), which was different from the vacuole membrane and yeast endosome localization of Dap1 in *S. cerevisiae* (10). However, DapB-GFP did not show localization in the ER or any other vacuole and instead localized in the nuclei and cytosol (Fig. 5A). Next, we used similar approaches to construct strains expressing Erg5-GFP (SJX26), Erg11A-GFP (SJX27), and Erg11B-GFP (SJX28). Each of these strains showed ER localization of the GFP-tagged protein (see Fig. S5B in the supplemental material), which was consistent with the previous finding that both Erg5 and Erg11 are ER-localized proteins (21, 26). To further examine whether DapA and DapC colocalized with Erg11, we constructed two doubly labeled strains derived from DapA-GFP or DapC-GFP strains by tagging the C terminus of Erg11A with red fluorescence protein (RFP); we named these strains SJX29 and SJX30. The dually labeled proteins were functional, and the strains expressing them showed normal growth phenotypes. Merged fluorescence microscopy studies indicated that Erg11A-RFP mainly colocalized with DapA-GFP, as well as with DapC-GFP, in the ER (Fig. 5B). The localization of DapA and DapC, along with Erg5 and Erg11, to the ER supports the idea that Dap members could interact closely with Erg5 and Erg11.

Dysfunction of Erg5 and Erg11 mediated by Dap is suppressed by exogenous hemin. Our findings described thus far have indicated that DapA dominantly controls azole susceptibility

by inducing dysfunction of Erg5 and Erg11 and that overexpression of these Erg proteins is capable of suppressing the *dapA* mutant defect. We wondered whether DapA affects the expression or the stability of the Erg5 and Erg11 proteins, because qRT-PCR data indicated that *dapA* could not affect the transcription levels of the *erg5* and *erg11* genes (see Fig. S6A in the supplemental material). To test this, two strains expressing a C-terminally GFP-tagged Erg5 or Erg11A protein, each under its native *erg* gene promoter, were constructed in the background of a *dapA* deletion strain and named SJX31 and SJX32, respectively. Interestingly, the levels of Erg11A and Erg5 that accumulated in the absence of *dapA* were significantly decreased, by 35% and 49%, respectively, compared with the levels in the parental control strains under the same culture conditions (Fig. 6A; see also Fig. S6C in the supplemental material). Because a strain expressing a C-terminally GFP-tagged Erg11B protein could not be successfully constructed using the native *erg* gene promoter, we next constructed such a strain using the *gpd* promoter (strain SJX33). Surprisingly, the deletion of *dapA* almost completely abolished the normal expression of Erg11B and resulted in the absence of a detectable full-length protein, but the analysis showed the existence of some small, degraded proteins (Fig. 6A). Consistent with this, the ER localization of Erg11B-GFP was also absent in the *dapA* deletion strain in 10 independent confirmed transformants. In contrast, a clear Erg11B-GFP signal with an ER localization was shown in the parental wild-type strain under the same cultural conditions (Fig. 6B). We next analyzed and compared the transcription levels of *erg11B* by RT-PCR, using tubulin as a loading control. Abundant transcription was clearly detected in both the mutant and its parental strains, indicating that the transcriptional level of *erg11B* was almost normal in the *dapA* deletion mutant compared with the level in the parental strain (see Fig. S6B). These results indicate that the requirement of DapA for the normal protein expression of Erg5 and Erg11A/B is most likely due to an effect on protein stabilization. Previous work in yeast suggested that endogenously synthesized heme, as well as exogenous hemin (an oxidized form

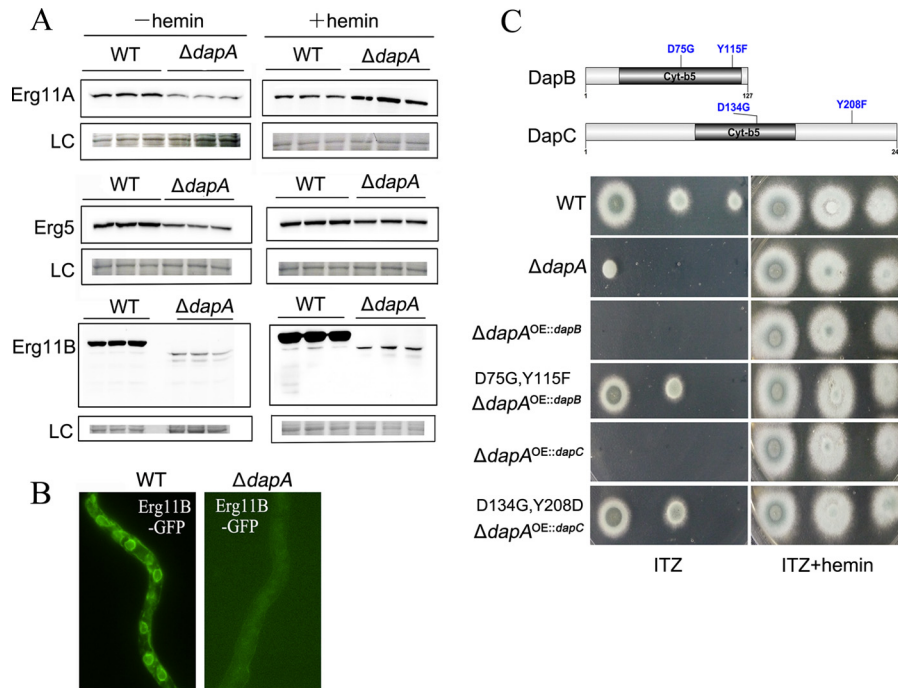


FIG 6 Dysfunction of Erg5 and Erg11 mediated by Dap proteins is suppressed by exogenous hemin. (A) Western blots show the protein expression of Erg11A/B and Erg5 in the $\Delta dapA$ and the parental wild-type strains with or without the addition of hemin (13 $\mu\text{g}/\text{ml}$), indicating that hemin could rescue the expression of Erg11A and Erg5 to a remarkable degree but could not rescue the expression defect of Erg11B in the $\Delta dapA$ mutant with the full-length deletion. (B) Comparison of Erg11B-GFP localization in the $\Delta dapA$ mutant and the parental wild-type strain as visualized by fluorescence microscopy. (C) Comparison of the susceptibility to ITZ of the indicated mutants with or without the addition of hemin (48 $\mu\text{g}/\text{ml}$) to the medium. (Top) Predicted structure and heme-binding sites of DapB and DapC.

of heme), regulates the cytochrome P450 protein Erg11p/Cyp51p (20). We next asked whether the expression and stability of Erg5 and Erg11 maintained by DapA are related to heme. To test this hypothesis, we cultured the aforementioned related strains in medium amended with exogenous hemin (protoporphyrin IX, containing a ferric iron ion), an oxidized version of heme with a function similar to that of heme B. Interestingly, after 24 h of incubation, the expression of both Erg5 and Erg11A in the $dapA$ deletion strains exhibited a remarkable recovery, to normal or increased levels, respectively, compared with the levels in the parental strains (Fig. 6A; see also Fig. S6D). Conversely, the addition of hemin was unable to rescue the expression of Erg11B at the predicted full-length size in the $\Delta dapA$ strain (Fig. 6A). The results suggest that hemin can bypass the requirement of DapA during the maintenance of Erg5 and Erg11A expression but not for Erg11B expression (Fig. 6A). Thus, it appears that DapA maintains the normal expression levels of the cytochrome P450 enzymes Erg5 and Erg11 in a heme-dependent manner.

To further test the biological importance of heme binding for DapA, we created a new strain with point mutations of two predicted heme-binding sites in DapA, changing the D at position 90 to G and the Y at position 138 to F [DapA^(D90G Y138F)], based on conserved sequence alignment information indicating that these sites are related to heme binding in yeast. Similar to the $\Delta dapA$ mutant, the DapA^(D90G Y138F) strain also showed a susceptibility phenotype in the presence of azole (see Fig. S7A in the supplemental material), suggesting that the defective heme-binding ability in DapA truly contributes the ITZ-hypersensitivity phenotype. The addition of hemin was able to restore the decreased azole suscep-

tibility in a dose-dependent manner, indicating that excess hemin can bypass the requirement of DapA. As DapB and DapC also possess the cytochrome *b*₅-like heme-binding domain, we further asked whether hemin could affect the azole susceptibility of the SJX13 ($\Delta dapA^{\text{OE}::dapB}$) and SJX15 ($\Delta dapA^{\text{OE}::dapC}$) strains. Our results showed that external hemin could rescue the hypersensitivity phenotype of the SJX13 and SJX15 strains (Fig. 6C). This phenomenon led us to deduce that the hypersensitivity phenotype induced by the overexpression of *dapB* and *dapC* is possibly related to the depletion of heme. To address this hypothesis, we created point mutations of two predicted heme-binding sites in each gene product, creating the DapB^(D75G Y115F) and DapC^(D134G Y208F) mutants, based on conserved sequence alignment information indicating that these sites are related to heme binding in yeast (20, 21). We then created overexpression mutants with these point-mutated alleles in the $\Delta dapA$ background to create strains SJX34 [OE::DapB^(D75G Y115F)] and SJX35 [OE::DapC^(D134G Y208F)]. Our results showed that placement of the OE::*dapB*^(D75G Y115F) or OE::*dapC*^(D134G Y208F) allele in a $\Delta dapA$ strain completely abolished the ITZ-hypersensitivity phenotype and instead resulted in strains with azole sensitivities that were intermediate between those of the $\Delta dapA$ strain and the wild type (Fig. 6C), indicating that the putative heme-binding ability of DapB or DapC truly contributes the ITZ-hypersensitivity phenotype. However, these mutants displayed azole sensitivities that were intermediate between those of the $\Delta dapA$ strain and the parental wild type. This suggests that, besides the heme binding motif, DapB and -C may have other motifs or domains that may also affect azole susceptibility, so that the site-directed mutants were

unable to show exactly the same phenotypes as strains with deletions of the respective full-length proteins.

Next, we investigated and compared the dose-dependent impacts of hemin addition on the azole sensitivities of the $\Delta dapA$, $\Delta dapA^{OE::dapB}$, and $\Delta dapA^{OE::dapC}$ strains. Our results showed that more hemin is required to rescue the azole susceptibility phenotype in strains SJX13 ($\Delta dapA^{OE::dapB}$) and SJX15 ($\Delta dapA^{OE::dapC}$), especially SJX13, than is required for rescue of the $\Delta dapA$ strain (see Fig. S7B in the supplemental material). These data suggest that the ITZ-hypersensitivity phenotype induced by overexpression of DapB or DapC is closely related to the depletion of hemin. Taken together, these results suggest that heme binding by DapB and DapC, in contrast to DapA heme binding, has a negative consequence for cytochrome P450 functionality, which likely explains the azole hypersensitivity of strains SJX13 ($\Delta dapA^{OE::dapB}$) and SJX15 ($\Delta dapA^{OE::dapC}$).

Virulence and the azole susceptibilities of Dap mutants in an immunocompromised mouse model of invasive pulmonary aspergillosis. To assess any impact of Dap proteins in an *in vivo* murine model, we examined virulence and the efficacy of azole therapy for selected Dap mutant strains, the $\Delta dapA$ and $\Delta dapA^{OE::dapB}$ mutants, as representative of the azole-hypersensitivity phenotype. Conidia were inoculated into each group of 10 immunocompromised mice, while the mice in the control group were inoculated with saline solution. The group infected by the $\Delta dapA$ mutant showed a mortality rate similar to those of the groups infected with the parental strain and the reconstituted strain (see Fig. S8A in the supplemental material). The histopathologic analysis of infected lungs from day 3 postinfection was consistent with these mortality data, showing no difference between strains (see Fig. S8B). However, the mice infected by strain SJX13 ($\Delta dapA^{OE::dapB}$) displayed significantly attenuated virulence compared to those infected by the parental wild-type strain according to Kaplan-Meier log rank analysis ($P < 0.001$) (Fig. 7A), suggesting that *dapB* overexpression contributes to the pathogenicity associated with the loss of *dapA* function. Through histopathologic analysis of infected lungs on day 3 postinfection, we found that mice infected with the parental strain A1160 had experienced extensive fungal growth. In contrast, only a small amount of fungal growth was observed in the strain SJX13-infected mice at the same time point, with the tissue samples containing poorly germinated and ungerminated conidia (Fig. 7C). We next sacrificed all of the SJX13 strain-infected mice to analyze the fungal burden measured by real-time PCR, which showed that the fungal load was significantly reduced ($P < 0.01$) in the strain SJX13-infected group compared to the load in the mice infected with the parental strain (Fig. 7B). Histopathological analyses on day 14 postinfection also confirmed that the fungal persistence and inflammation in mice infected with the SJX13 strain was remarkably decreased compared to those in mice infected with the parental strain A1160 (Fig. 7C).

Next, we verified whether strain SJX13 also conferred hypersensitivity to azoles in an immunocompromised mouse model of invasive pulmonary aspergillosis. ITZ was given via intragastric administration, first on day 1 post-fungal infection and again on day 2 post-fungal infection. Our results showed that ITZ administration was capable of increasing the survival rate in mice compared with that of the group not given ITZ therapy, indicating that ITZ therapy in our immunocompromised mouse model was successful. Notably, *in vivo* data confirmed that strain SJX13 was eas-

ily treatable with azoles in an immunocompromised mouse model of invasive pulmonary aspergillosis, resulting in survival of 9/10 (90%) mice at 14 days postinfection (Fig. 7A). Kaplan-Meier log rank analysis showed there was a significant difference between these two groups ($P < 0.001$), further suggesting that the survival rate of mice infected with the SJX13 strain was significantly higher than that of the mice infected with the control parental wild-type strain after ITZ administration.

These *in vivo* data support a role for Dap proteins in mediating azole susceptibility and virulence in *A. fumigatus*.

DISCUSSION

Dramatic increases in the incidence of aspergillosis caused primarily by *A. fumigatus* have occurred in recent years, primarily due to an increase in the use of immunosuppressive therapies (27, 28). Azole antifungals bind very weakly to mammalian cytochrome P450, which considerably reduces the toxicity of the drug in humans (29). Thus, to date, most antifungals are azole based, and azoles are currently the mainstay of antifungal treatment both in agricultural and in clinical settings (30, 31). Many biochemistry studies have verified that the free nitrogen of azole molecules is able to compete for oxygen with the catalytic heme of cytochrome P450 enzymes to inhibit the synthesis of ergosterol in fungal membranes (32). The lack of ergosterol alters membrane fluidity and steric relationships for selected membrane-associated enzymes and results in the accumulation of phospholipids and unsaturated fatty acids within the fungal cells (33–35). Although *Aspergillus* species are generally susceptible to azoles, intrinsic and acquired resistance, particularly in the most common pathogenic species, *A. fumigatus*, is well documented and worrisomely on the rise (36, 37). A thorough understanding of the drug resistance mechanisms of this fungus requires extensive exploration. In this study, we uncover a family of three conserved cytochrome *b*₅-like heme-binding proteins, DapA, -B, and -C, that regulate the functionality of three critical ergosterol-biosynthetic P450 enzymes, Erg5 and Erg11A and -B. In contrast, overexpression of DapB and DapC causes dysfunction of Erg5 and Erg11, resulting in abnormal accumulation of sterol intermediates and further accentuating the sensitivity of $\Delta dapA$ mutants to azoles. Our studies reveal that heme binding lies at the heart of this regulation, where DapA promotes Erg5 and Erg11 functionality, while DapB and DapC inhibit Erg5 and Erg11 activities. Thus, our finding provides the first characterization of the Dap family in *A. fumigatus* and also gives insight to understand that the Dap family members act differently on sterol biosynthesis. A putative working model of this mechanism is presented in Fig. 8. The azole-sensitive phenotypes of Dap mutants revealed in this study yield possible avenues to uncover alternative fungal-specific cellular targets.

Functions for multiple Dap homologs. Our genome-scale homologue search shows that most fungal species encode three Dap proteins. Interestingly, the *C. albicans* genome contains four copies (two DapC proteins), which is possibly due to a recent gene duplication event. The *Kluyveromyces lactis* and *Ashbya gossypii* genomes possess two Dap protein copies (DapA and -C), while the *S. cerevisiae*, *S. pombe*, and *Candida glabrata* genomes only encode DapA, which might be due to independent losses of DapB and -C during convergent evolution.

Although all three *dap* genes in *A. fumigatus* showed increased expression in an azole-dependent manner, the proteins exhibited opposite roles in azole sensitivity, where DapA promotes resis-

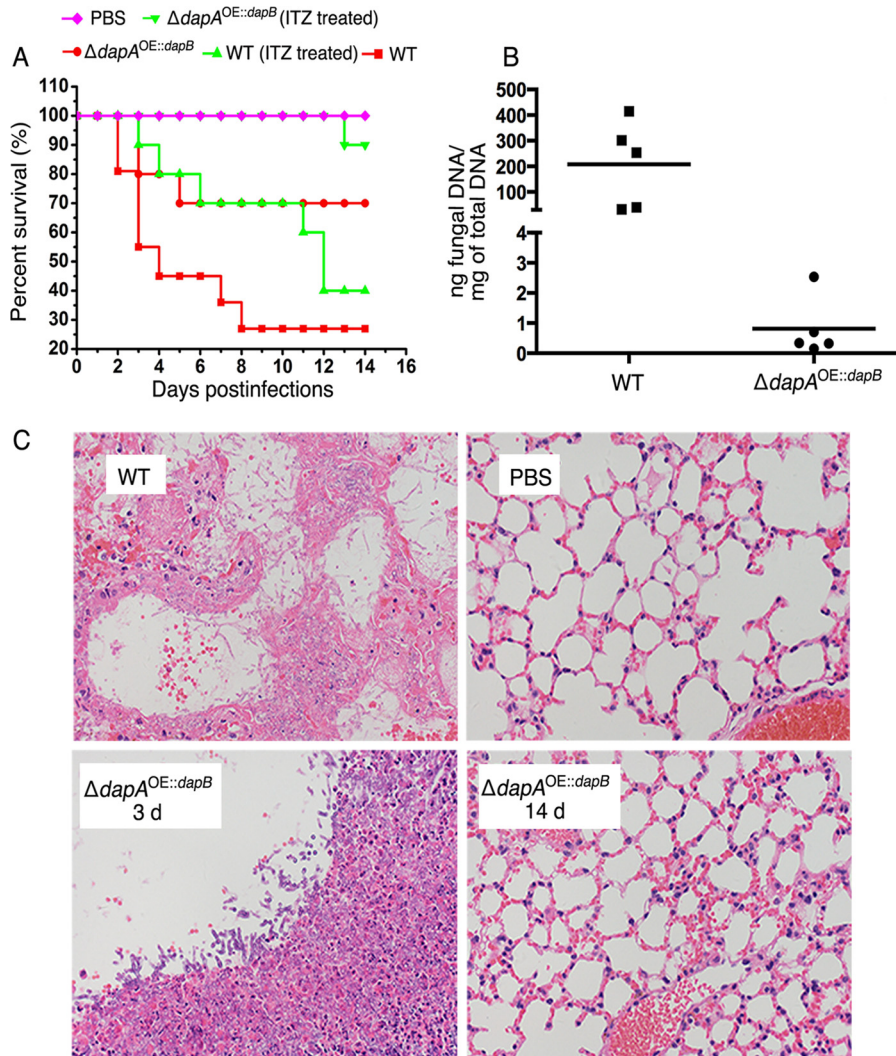


FIG 7 Virulence and azole susceptibilities of Dap mutants in an immunocompromised mouse model of invasive pulmonary aspergillosis. (A) The cyclophosphamide mouse model was used for virulence analysis. The mice were immunosuppressed as described in Materials and Methods, infected, and observed for mortality for 14 days. PBS was used for the mock-infection control group. In the susceptibility comparison of the $\Delta dapA^{OE::dapB}$ (SjX13) strain and the parental strain, ITZ was first given on day 1 post-fungal infection and again on day 2 post-fungal infection via intragastric administration. The mice infected with strain SjX13 ($\Delta dapA^{OE::dapB}$) displayed attenuated virulence compared to those infected with the parental wild-type strain as determined by Kaplan-Meier log rank analysis ($P < 0.001$). After ITZ administration, the survival rate of the mice infected with the SjX13 strain was significantly higher than that of the mice infected with the control parental wild-type strain (log rank test, $P < 0.001$). (B) qRT-PCR was done to determine the amount of fungal DNA in $\Delta dapA^{OE::dapB}$ strain-infected mice, which survived to the end of the experiment (day 14), and in parental-strain-infected mice, which became moribund or died during the 14 days postinfection. Statistical analysis was performed using analysis of variance (ANOVA). Statistical significance was accepted at a P value of < 0.01 . The horizontal lines represent the average level for tested groups. (C) Histopathology of representative lung sections in infected mice. Tissue samples were stained with periodic acid-Schiff stain. No detectable fungal lesions or fungal burden was observed in surviving mice on day 14 postinfection.

tance to azoles and DapB and DapC promote sensitivity. This was determined by growth studies of both deletion and overexpression on azole-amended media. The most sensitive strains were those in which overexpression alleles of *dapB* or *dapC* were coupled with a *dapA* deletion, both *in vitro* and *in vivo* (Fig. 3 and 7A). DapC seems to play a somewhat stronger role in azole response than DapB, as its deletion, unlike that of DapB, led to enhanced resistance to azoles (Fig. 2). In comparison, mutants with double deletions of *dapA* and *dapB* or *dapA* and *dapC* each showed an azole susceptibility phenotype similar to that of the *dapA* single deletion mutant, suggesting that *dapA* may dominantly control the azole response and that the deletion of *dapB* or *dapC* is unable to sup-

press the defective response of the *dapA* mutant (Fig. 3A). These data suggest that all three Dap proteins function to balance the stress response in fungal cells.

Dap family proteins coordinately regulate cytochrome P450 activities. Studies assessing the mechanisms regulating ergosterol enzyme functionality in *A. fumigatus* are quite limited (38). It is clear that cytochrome *b₅* has a number of influences on the different enzyme systems (23). Most of the systems in which cytochrome *b₅* participates, particularly those involved in lipid metabolism, are complexed with cytochrome P450s as an electron transfer component (23). Thus, it is possible that Dap proteins coordinately affect electron transfer to regulate cytochrome P450

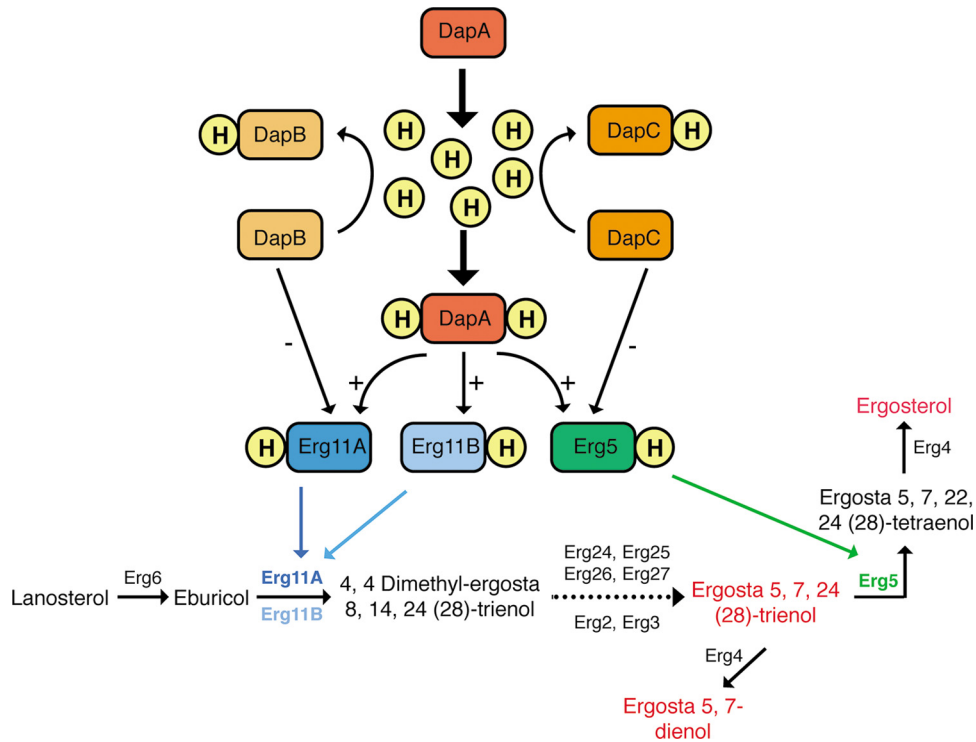


FIG 8 Schematic model of Dap family function. DapA activates Erg11A/B and Erg5 through chaperoning heme (H) to Erg11A/B and Erg5 and stabilizing Erg11A/B-heme and Erg5-heme complexes and, thus, regulates ergosterol biosynthesis and azole susceptibility. DapB and -C are capable of reducing the activities of Erg5 and Erg11 directly or through depletion of heme. DapB and DapC may also directly repress Erg11 and Erg5 cytochrome P450 activities.

activities. In yeasts, there are contradictory conclusions about whether the hemoprotein Dap1 forms a stable complex with the cytochrome P450 enzyme Cyp51A (only with encoded Cyp51A/Erg11A but without Erg11B paralog) through Dap1p heme binding (21, 39). In comparison, our data support the idea that *dapA* deletion is able to sharply decrease the stability of Erg5 and Erg11A and results in the degradation of Erg11B. When mutants with deletion of *dapA* and overexpression of *dapB* or *dapC* in combination with predicted heme-binding site mutations were used in a rescue experiment performed by adding hemin, the results suggested the differential roles induced by the Dap family. Thus, our findings suggest that heme binding is a critical component of Dap protein interaction not only with Erg11A/B but also with Erg5 proteins. In addition, loss of DapA function enhances azole susceptibility through loss of cytochrome P450 activity, particularly Erg11A/B. In contrast, DapB and DapC binding of heme pools reduces cytochrome P450 functionality. The colocalization of DapA and DapC with Erg11/Erg5 (Fig. 5) would enhance these interactions, possibly through a mechanism where DapA allows transfer of heme to Erg P450 proteins, while DapB and DapC irreversibly hold heme to suppress the cytochrome P450 activities. In addition, multiple copies of *erg5* could suppress the abnormal accumulation of ergosta-5,7-dienol in *dapA* deletion mutants but could not affect ITZ susceptibility. In contrast, in the absence of *dapA*, multiple copies of *erg11A* and *erg11B* significantly decreased the efficacy of ITZ but were unable to decrease the accumulation of ergosta-5,7-dienol (Fig. 4C and D). These data suggest that DapA affects the functions of Erg5 and Erg11 independently. In addition, *dapB* or *dapC* overexpression in the absence of *dapA* led to an ITZ-hypersensitivity phenotype, indicating that DapB and

-C negatively regulate the activities of both Erg5 and Erg11. These findings collectively indicate that the Dap family affects the activities of three P450 enzymes, Erg11A, Erg11B, and Erg5. Dap proteins not only affect the C-22 desaturase encoded by *erg5* but also regulate the normal functions of the lanosterol demethylase encoded by *erg11A* and *erg11B* during the process of ergosterol biosynthesis.

Numerous azole-resistant *A. fumigatus* isolates have been found worldwide, most of which are due to point mutations in Erg11A or an alteration in the expression of its gene (40–43). This observation underscores the basic inadequacy of drugs targeting *A. fumigatus* Erg11A and emphasizes the urgent need for new antifungal targets. Pharmaceutical companies continue to be actively involved in the search for new anti-*Aspergillus* drugs by investigating new or revisited potential cellular targets. Thus, our new insights into the specific and complicated Dap regulatory system that promotes balanced ergosterol biosynthesis may have broad therapeutic ramifications beyond classic azole antifungals.

Dap proteins and virulence. Mice infected with the Δ *dapA* mutant showed a mortality rate similar to that of mice infected with its parental strain, while the *dapB*-overexpressing *dapA* deletion mutant strain showed attenuated virulence. We wondered, what is the reason? Whereas overexpression of *dapB* in the Δ *dapA* background had no remarkable phenotype in the absence of azole drug treatment, the mutant presented a hypersensitive phenotype on ITZ-amended medium (Fig. 3A). The sterol profile from strain SJX13 (Δ *dapA*^{OE::dapB}) showed increased peaks of two intermediate fractions, as well as a decreased peak of the main component, ergosterol, compared with the profile of the parental strain (Fig. 4B). These data indicate that strain SJX13 (Δ *dapA*^{OE::dapB})

has an abnormal or defective ergosterol biosynthesis pathway. Previous studies have verified that there might be a tight link between ergosterol biosynthesis and iron acquisition ability, which is a major factor in host defense against the pathogen (44–46). To test whether the *dapB* overexpression in the *dapA* deletion mutant could result in a defect in iron acquisition ability, the $\Delta dapA^{OE::dapB}$ mutant was inoculated onto minimal medium. It appeared to have robust hyphal growth and conidiation even though it probably displayed a slightly smaller colony size than the parental strain. In comparison, when inoculated onto minimal medium containing the iron chelator bathophenanthroline disulfonate (BPS; 200 μ M), the mutant displayed very severe growth defects compared to the growth of the parental strain (see Fig. S8C in the supplemental material), indicating that the $\Delta dapA^{OE::dapB}$ mutant had an impaired iron acquisition ability, especially under the low-iron cultural condition, while there was no detectable difference between the $\Delta dapA$ mutant and its parental strain under the iron-limited cultural condition. These data also suggest the possibility that the main reason for the attenuated virulence in the mouse model is the damaged iron acquisition in the $\Delta dapA^{OE::dapB}$ mutant. It seems probable that deprivation of hemin by overexpression of DapB leads to dysfunction of cellular mechanisms other than DapA function. Moreover, we found that inactivated DapA combined with activated DapB yields an *A. fumigatus* mutant that is easily treatable with azoles in an immunocompromised mouse model of invasive pulmonary aspergillosis.

MATERIALS AND METHODS

Additional details on the materials and methods used can be found in Text S1 in the supplemental material.

Strains, media, and culture conditions. The *A. fumigatus* strains used in this study are listed in Table S1 in the supplemental material. Mutant strains were constructed as described in detail in Text S1.

Antifungal susceptibility testing. Susceptibility testing of all *dap* mutants and the parental strains against the antifungal drugs ITZ and VOR was performed using solid and liquid media. MIC values are based on E-test strip assays (47).

Microscopy and live-cell imaging. Fluorescence localization and image processing for fungi expressing DapA-GFP, DapB-GFP, and DapC-GFP and Erg11-RFP were performed as described in reference 48.

Western blotting. The expression levels of GFP and RFP fusion proteins were determined by probing Western blots with the respective antibody (Roche) and developing them by enhanced chemiluminescence (ECL; Amersham) as described previously (49). Signal intensity was calculated by using a gel imaging system, and statistical analysis was performed using analysis of variance (ANOVA). Statistical significance is accepted at a *P* value of <0.05.

Total sterol extraction and HPLC-MS analysis. The sterols extracted from *A. fumigatus* strains were analyzed using HPLC (Agilent Technologies) and detected at 280 nm on a AQ C₁₈ column (250 mm by 4.6 mm with a 5- μ m particle size). HPLC-MS/MS was carried out using a Fourier transform ion cyclotron resonance (FT-ICR) mass spectrometer with a reverse-phase C₁₈ column (AQ C₁₈ column, 4.6 mm by 250 mm with a 5- μ m particle size).

RNA preparation. Total RNA was isolated using TRIzol (catalog number 15596-025; Invitrogen), following the manufacturer's instructions.

Murine virulence and the azole susceptibility assays. The immunocompromised mouse model for invasive pulmonary aspergillosis was described previously (50). Briefly, white female ICR mice (6 to 8 weeks old, 22 to 25 g) were given intraperitoneal injections of cyclophosphamide (150 mg/kg of body weight) on days 3 and 1 relative to infection and a subcutaneous injection of hydrocortisone acetate (40 mg/kg of body

weight) on day 1. Statistical analysis of survival was performed using Kaplan-Meier log rank analysis. Statistical significance is accepted at a *P* value of <0.01. All animal experiments in this study were performed according to the Guide for the Care and Use of Laboratory Animals of the U.S. National Institutes of Health (51). The animal experimental protocol was approved by the Animal Care and Use Committee of Nanjing Normal University, China (permit no. 2090658) according to the governmental guidelines for animal care.

SUPPLEMENTAL MATERIAL

Supplemental material for this article may be found at <http://mbio.asm.org/lookup/suppl/doi:10.1128/mBio.01919-15/-/DCSupplemental>.

Figure S1, TIF file, 2.8 MB.
Figure S2, TIF file, 0.4 MB.
Figure S3, TIF file, 2.4 MB.
Figure S4, TIF file, 1.4 MB.
Figure S5, TIF file, 1.4 MB.
Figure S6, TIF file, 0.3 MB.
Figure S7, TIF file, 1 MB.
Figure S8, TIF file, 2.5 MB.
Table S1, DOC file, 0.1 MB.
Text S1, DOC file, 0.08 MB.

ACKNOWLEDGMENTS

This work was financially supported by grants from the National Natural Science Foundation of China (NSFC81330035) to L.L., the Special Fund for the Doctoral Program of Higher Education of China (no. 20123207110012) to L.L., Innovation Project for College Graduates of Jiangsu Province (grant no. CXZZ13_0415), Excellent Doctoral Dissertation Special Fund of Nanjing Normal University (grant no. 181200002140) to J.S., the Priority Academic Program Development (PAPD) of Jiangsu Higher Education Institutions, and the NIH R01 Al065728-01 to N.P.K.

A. fumigatus strain Af1160 was obtained from FGSC (<http://www.fg-sc.net>).

FUNDING INFORMATION

The Special Fund for the Doctoral Program of Higher Education of China provided funding to Ling Lu under grant number No. 20123207110012. Innovation Project for College Graduates of Jiangsu Province provided funding to Jinxing Song under grant number No. CXZZ13_0415. Excellent Doctoral Dissertation Special Fund of Nanjing Normal University provided funding to Jinxing Song under grant number No. 181200002140.

This work was funded by National Natural Science Foundation of China (NSFC) under grant NSFC81330035 and by NIH R01 Al065728-01 to N.P.K. The funders had no role in study design, data collection and interpretation, or the decision to submit the work for publication.

REFERENCES

- Caspeta L, Chen Y, Ghiaci P, Feizi A, Buskov S, Hallström BM, Petranovic D, Nielsen J. 2014. Biofuels. Altered sterol composition renders yeast thermotolerant. *Science* 346:75–78. <http://dx.doi.org/10.1126/science.1258137>.
- Sáenz JP, Sezgin E, Schwillie P, Simons K. 2012. Functional convergence of hopanoids and sterols in membrane ordering. *Proc Natl Acad Sci U S A* 109:14236–14240. <http://dx.doi.org/10.1073/pnas.1212141109>.
- Hodzic A, Rappolt M, Amenitsch H, Laggner P, Pabst G. 2008. Differential modulation of membrane structure and fluctuations by plant sterols and cholesterol. *Biophys J* 94:3935–3944. <http://dx.doi.org/10.1529/biophysj.107.123224>.
- Dupont S, Beney L, Ferreira T, Gervais P. 2011. Nature of sterols affects plasma membrane behavior and yeast survival during dehydration. *Biochim Biophys Acta* 1808:1520–1528. <http://dx.doi.org/10.1016/j.bbame.2010.11.012>.
- Zarnowski R, Westler WM, Lacmbouh GA, Marita JM, Bothe JR, Bernhardt J, Lounes-Hadj Sahraoui A, Fontaine J, Sanchez H, Hatfield

- RD, Ntambi JM, Nett JE, Mitchell AP, Andes DR. 2014. Novel entries in a fungal biofilm matrix encyclopedia. *mBio* 5(4):e01333-14. <http://dx.doi.org/10.1128/mBio.01333-14>.
6. Mor V, Rella A, Farnoud AM, Singh A, Munshi M, Bryan A, Naseem S, Konopka JB, Ojima I, Bullesbach E, Ashbaugh A, Linke MJ, Cushion M, Collins M, Ananthula HK, Sallans L, Desai PB, Wiederhold NP, Fothergill AW, Kirkpatrick WR, Patterson T, Wong LH, Sinha S, Giaefer G, Nislow C, Flaherty P, Pan XW, Cesar GV, Tavares PD, Frases S, Miranda K, Rodrigues ML, Luberto C, Nimrichter L, Del Poeta M. 2015. Identification of a new class of antifungals targeting the synthesis of fungal sphingolipids. *mBio* 6:e00647-15. <http://dx.doi.org/10.1128/mBio.00647-15>.
 7. Matyash V, Entchev EV, Mende F, Wilsch-Braüninger M, Thiele C, Schmidt AW, Knölker HJ, Ward S, Kurzchalia TV. 2004. Sterol-derived hormone(s) controls entry into diapause in *Caenorhabditis elegans* by consecutive activation of DAF-12 and DAF-16. *PLoS Biol* 2:e280. <http://dx.doi.org/10.1371/journal.pbio.0020280>.
 8. Yoshida Y, Aoyama Y. 1987. Interaction of azole antifungal agents with cytochrome P-450_{14DM} purified from *Saccharomyces cerevisiae* microsomes. *Biochem Pharmacol* 36:229–235. [http://dx.doi.org/10.1016/0006-2952\(87\)90694-0](http://dx.doi.org/10.1016/0006-2952(87)90694-0).
 9. Hannemann F, Bichet A, Ewen KM, Bernhardt R. 2007. Cytochrome P450 systems—biological variations of electron transport chains. *Biochim Biophys Acta* 1770:330–344. <http://dx.doi.org/10.1016/j.bbagen.2006.07.017>.
 10. Craven RJ, Mallory JC, Hand RA. 2007. Regulation of iron homeostasis mediated by the heme-binding protein Dap1 (damage resistance protein 1) via the p450 protein Erg11/Cyp51. *J Biol Chem* 282:36543–36551. <http://dx.doi.org/10.1074/jbc.M706770200>.
 11. Mellado E, Diaz-Guerra TM, Cuenca-Estrella M, Rodriguez-Tudela JL. 2001. Identification of two different 14- α sterol demethylase-related genes (*cyp51A* and *cyp51B*) in *Aspergillus fumigatus* and other *Aspergillus* species. *J Clin Microbiol* 39:2431–2438. <http://dx.doi.org/10.1128/JCM.39.7.2431-2438.2001>.
 12. Mellado E, Garcia-Effron G, Buitrago MJ, Alcazar-Fuoli L, Cuenca-Estrella M, Rodriguez-Tudela JL. 2005. Targeted gene disruption of the 14- α sterol demethylase (*cyp51A*) in *Aspergillus fumigatus* and its role in azole drug susceptibility. *Antimicrob Agents Chemother* 49:2536–2538. <http://dx.doi.org/10.1128/AAC.49.6.2536-2538.2005>.
 13. Warrilow AG, Melo N, Martel CM, Parker JE, Nes WD, Kelly SL, Kelly DE. 2010. Expression, purification, and characterization of *Aspergillus fumigatus* sterol 14- α demethylase (CYP51) isoenzymes A and B. *Antimicrob Agents Chemother* 54:4225–4234. <http://dx.doi.org/10.1128/AAC.00316-10>.
 14. Hu W, Sillaots S, Lemieux S, Davison J, Kauffman S, Breton A, Linteau A, Xin C, Bowman J, Becker J, Jiang B, Roemer T. 2007. Essential gene identification and drug target prioritization in *Aspergillus fumigatus*. *PLoS Pathog* 3:e24. <http://dx.doi.org/10.1371/journal.ppat.0030024>.
 15. Snelders E, Camps SM, Karawajczyk A, Rijs AJ, Zoll J, Verweij PE, Melchers WJ. 2015. Genotype–phenotype complexity of the TR 46/Y121F/T289A *cyp51A* azole resistance mechanism in *Aspergillus fumigatus*. *Fungal Genet Biol* 82:129–135. <http://dx.doi.org/10.1016/j.fgb.2015.06.001>.
 16. Abdolrasouli A, Rhodes J, Beale MA, Hagen F, Rogers TR, Chowdhary A, Meis JF, Armstrong-James D, Fisher MC. 2015. Genomic context of azole resistance mutations in *Aspergillus fumigatus* determined using whole-genome sequencing. *mBio* 6:e00536-15. <http://dx.doi.org/10.1128/mBio.00536-15>.
 17. Gollapudy R, Ajmani S, Kulkarni SA. 2004. Modeling and interactions of *Aspergillus fumigatus* lanosterol 14- α demethylase “A” with azole antifungals. *Bioorg Med Chem* 12:2937–2950. <http://dx.doi.org/10.1016/j.bmc.2004.03.034>.
 18. Onyewu C, Blankenship JR, Del Poeta M, Heitman J. 2003. Ergosterol biosynthesis inhibitors become fungicidal when combined with calcineurin inhibitors against *Candida albicans*, *Candida glabrata*, and *Candida krusei*. *Antimicrob Agents Chemother* 47:956–964. <http://dx.doi.org/10.1128/AAC.47.3.956-964.2003>.
 19. Hand RA, Jia N, Bard M, Craven RJ. 2003. *Saccharomyces cerevisiae* Dap1p, a novel DNA damage response protein related to the mammalian membrane-associated progesterone receptor. *Eukaryot Cell* 2:306–317. <http://dx.doi.org/10.1128/EC.2.2.306-317.2003>.
 20. Mallory JC, Crudden G, Johnson BL, Mo C, Pierson CA, Bard M, Craven RJ. 2005. Dap1p, a heme-binding protein that regulates the cytochrome P450 protein Erg11p/Cyp51p in *Saccharomyces cerevisiae*. *Mol Cell Biol* 25:1669–1679. <http://dx.doi.org/10.1128/MCB.25.5.1669-1679.2005>.
 21. Hughes AL, Powell DW, Bard M, Eckstein J, Barbuch R, Link AJ, Espenshade PJ. 2007. Dap1/PGRMC1 binds and regulates cytochrome P450 enzymes. *Cell Metab* 5:143–149. <http://dx.doi.org/10.1016/j.cmet.2006.12.009>.
 22. Meyer C, Schmid R, Scriba PC, Wehling M. 1996. Purification and partial sequencing of high-affinity progesterone-binding site(s) from porcine liver membranes. *Eur J Biochem* 239:726–731. <http://dx.doi.org/10.1111/j.1432-1033.1996.0726u.x>.
 23. Schenkman JB, Jansson I. 2003. The many roles of cytochrome b(5). *Pharmacol Ther* 97:139–152. [http://dx.doi.org/10.1016/S0163-7258\(02\)00327-3](http://dx.doi.org/10.1016/S0163-7258(02)00327-3).
 24. Blosser SJ, Cramer RA. 2012. SREBP-dependent triazole susceptibility in *Aspergillus fumigatus* is mediated through direct transcriptional regulation of *erg11A* (*cyp51A*). *Antimicrob Agents Chemother* 56:248–257. <http://dx.doi.org/10.1128/AAC.05027-11>.
 25. Sun X, Wang W, Wang K, Yu X, Liu J, Zhou F, Xie B, Li S. 2013. Sterol C-22 desaturase ERG5 mediates the sensitivity to antifungal azoles in *Neurospora crassa* and *Fusarium verticillioides*. *Front Microbiol* 4:127. <http://dx.doi.org/10.3389/fmicb.2013.00127>.
 26. Homma K, Yoshida Y, Nakano A. 2000. Evidence for recycling of cytochrome P450 sterol 14-demethylase from the *cis*-Golgi compartment to the endoplasmic reticulum (ER) upon saturation of the ER-retention mechanism. *J Biochem* 127:747–754. <http://dx.doi.org/10.1093/oxfordjournals.jbchem.a022666>.
 27. Wingard JR. 2005. The changing face of invasive fungal infections in hematopoietic cell transplant recipients. *Curr Opin Oncol* 17:89–92. <http://dx.doi.org/10.1097/01.cco.0000152975.65477.7c>.
 28. Ascioğlu S, Rex JH, de Pauw B, Bennett JE, Bille J, Crokaert F, Denning DW, Donnelly JP, Edwards JE, Erjavec Z, Fiere D, Lortholary O, Maertens J, Meis JF, Patterson TF, Ritter J, Selleslag D, Shah PM, Stevens DA, Walsh TJ, Coopera IFI. 2002. Defining opportunistic invasive fungal infections in immunocompromised patients with cancer and hematopoietic stem cell transplants: an international consensus. *Clin Infect Dis* 34:7–14. <http://dx.doi.org/10.1086/323335>.
 29. Georgopapadakou NH. 1998. Antifungals: mechanism of action and resistance, established and novel drugs. *Curr Opin Microbiol* 1:547–557. [http://dx.doi.org/10.1016/S1369-5274\(98\)80087-8](http://dx.doi.org/10.1016/S1369-5274(98)80087-8).
 30. Lass-Flörl C. 2011. Triazole antifungal agents in invasive fungal infections: a comparative review. *Drugs* 71:2405–2419. <http://dx.doi.org/10.2165/11596540-000000000-00000>.
 31. Verweij PE, Kema GH, Zwaan B, Melchers WJ. 2013. Triazole fungicides and the selection of resistance to medical triazoles in the opportunistic mould *Aspergillus fumigatus*. *Pest Manag Sci* 69:165–170. <http://dx.doi.org/10.1002/ps.3390>.
 32. White TC, Marr KA, Bowden RA. 1998. Clinical, cellular, and molecular factors that contribute to antifungal drug resistance. *Clin Microbiol Rev* 11:382–402.
 33. Mo C, Valachovic M, Randall SK, Nickels JT, Bard M. 2002. Protein-protein interactions among C-4 demethylation enzymes involved in yeast sterol biosynthesis. *Proc Natl Acad Sci U S A* 99:9739–9744. <http://dx.doi.org/10.1073/pnas.112202799>.
 34. Pichler H, Gaigg B, Hrastnik C, Achleitner G, Kohlwein SD, Zellnig G, Perktold A, Daum G. 2001. A subfraction of the yeast endoplasmic reticulum associates with the plasma membrane and has a high capacity to synthesize lipids. *Eur J Biochem* 268:2351–2361. <http://dx.doi.org/10.1046/j.1432-1327.2001.02116.x>.
 35. Laude AJ, Prior IA. 2004. Plasma membrane microdomains: organization, function and trafficking. *Mol Membr Biol* 21:193–205. <http://dx.doi.org/10.1080/09687680410001700517>.
 36. Arendrup MC. 2014. Update on antifungal resistance in *Aspergillus* and *Candida*. *Clin Microbiol Infect* 20(Suppl 6):42–48. <http://dx.doi.org/10.1111/1469-0691.12513>.
 37. Chowdhary A, Sharma C, Hagen F, Meis JF. 2014. Exploring azole antifungal drug resistance in *Aspergillus fumigatus* with special reference to resistance mechanisms. *Future Microbiol* 9:697–711. <http://dx.doi.org/10.2217/fmb.14.27>.
 38. Ferreira ME, Colombo AL, Paulsen I, Ren Q, Wortman J, Huang J, Goldman MH, Goldman GH. 2005. The ergosterol biosynthesis pathway, transporter genes, and azole resistance in *Aspergillus fumigatus*. *Med Mycol* 43(Suppl 1):S313–S319.

39. Thompson AM, Reddi AR, Shi X, Goldbeck RA, Moënne-Loccoz P, Gibney BR, Holman TR. 2007. Measurement of the heme affinity for yeast Dap1p, and its importance in cellular function. *Biochemistry* 46: 14629–14637. <http://dx.doi.org/10.1021/bi7013739>.
40. Howard SJ, Webster I, Moore CB, Gardiner RE, Park S, Perlin DS, Denning DW. 2006. Multi-azole resistance in *Aspergillus fumigatus*. *Int J Antimicrob Agents* 28:450–453. <http://dx.doi.org/10.1016/j.ijantimicag.2006.08.017>.
41. Mann PA, Parmegiani RM, Wei S-Q, Mendrick CA, Li X, Loebenberg D, DiDomenico B, Hare RS, Walker SS, McNicholas PM. 2003. Mutations in *Aspergillus fumigatus* resulting in reduced susceptibility to posaconazole appear to be restricted to a single amino acid in the cytochrome P450 14 alpha-demethylase. *Antimicrob Agents Chemother* 47:577–581. <http://dx.doi.org/10.1128/AAC.47.2.577-581.2003>.
42. Mellado E, Garcia-Effron G, Alcázar-Fuoli L, Melchers WJ, Verweij PE, Cuenca-Estrella M, Rodríguez-Tudela JL. 2007. A new *Aspergillus fumigatus* resistance mechanism conferring in vitro cross-resistance to azole antifungals involves a combination of cyp51A alterations. *Antimicrob Agents Chemother* 51:1897–1904. <http://dx.doi.org/10.1128/AAC.01092-06>.
43. Chen J, Li H, Li R, Bu D, Wan Z. 2005. Mutations in the cyp51A gene and susceptibility to itraconazole in *Aspergillus fumigatus* serially isolated from a patient with lung aspergilloma. *J Antimicrob Chemother* 55:31–37. <http://dx.doi.org/10.1093/jac/dkh507>.
44. Blatzer M, Barker BM, Willger SD, Beckmann N, Blosser SJ, Cornish EJ, Mazurie A, Grahl N, Haas H, Cramer RA. 2011. SREBP coordinates iron and ergosterol homeostasis to mediate triazole drug and hypoxia responses in the human fungal pathogen *Aspergillus fumigatus*. *PLoS Genet* 7:e1002374. <http://dx.doi.org/10.1371/journal.pgen.1002374>.
45. Marvig RL, Damkær S, Khademi SM, Markussen TM, Molin S, Jelsbak L. 2014. Within-host evolution of *Pseudomonas aeruginosa* reveals adaptation toward iron acquisition from hemoglobin. *mBio* 5:e00966-14. <http://dx.doi.org/10.1128/mBio.00966-14>.
46. Hu G, Chen SH, Qiu J, Bennett JE, Myers TG, Williamson PR. 2014. Microevolution during serial mouse passage demonstrates FRE3 as a virulence adaptation gene in *Cryptococcus neoformans*. *mBio* 5:e00941-14. <http://dx.doi.org/10.1128/mBio.00941-14>.
47. Liu F-F, Pu L, Zheng Q-Q, Zhang Y-W, Gao R-S, Xu X-S, Zhang S-Z, Lu L. 2015. Calcium signaling mediates antifungal activity of triazole drugs in the aspergilli. *Fungal Genet Biol* 81:182–190. <http://dx.doi.org/10.1016/j.fgb.2014.12.005>.
48. Zhong G, Wei W, Guan Q, Ma Z, Wei H, Xu X, Zhang S, Lu L. 2012. Phosphoribosyl pyrophosphate synthetase, as a suppressor of the sepH mutation in *Aspergillus nidulans*, is required for the proper timing of septation. *Mol Microbiol* 86:894–907. <http://dx.doi.org/10.1111/mmi.12026>.
49. Zhong GW, Jiang P, Qiao WR, Zhang YW, Wei WF, Lu L. 2014. Protein phosphatase 2A (PP2A) regulatory subunits para and PabA orchestrate septation and conidiation and are essential for PP2A activity in *Aspergillus nidulans*. *Eukaryot Cell* 13:1494–1506. <http://dx.doi.org/10.1128/EC.00201-14>.
50. Jiang H, Shen Y, Liu W, Lu L. 2014. Deletion of the putative stretch-activated ion channel Mid1 is hypervirulent in *Aspergillus fumigatus*. *Fungal Genet Biol* 62:62–70. <http://dx.doi.org/10.1016/j.fgb.2013.11.003>.
51. National Research Council. 1996. Guide for the Care and Use of Laboratory Animals. National Academies Press, Washington, DC.